Crystallization of binary linear polyethylene blends

J. M. Rego Lopez*, M. T. Conde Braña, B. Terselius and U. W. Gedde†

Department of Polymer Technology, The Royal Institute of Technology, S-100 44 Stockholm, Sweden

Crystallization of binary mixtures of sharp linear polyethylene (LPE) fractions ($M_w = 2500$, 11 000, 22 000 and 66 000) has been studied directly by differential scanning calorimetry (d.s.c.) and hot stage polarized microscopy and indirectly by transmission electron microscopy (TEM). Three types of crystallization have been observed: (a) at high temperatures single (high molecular weight) component crystallization occurs. Data for the fold surface free energy obtained from linear growth rate data supports the view that the nature of the fold surface of the dominant lamellae is related only to the molecular weight of the crystallizing component and is not affected by the composition of the melt. A composition-induced shift occurs for the axialite–spherulite transition temperature for the L66 blends which can be explained by a change in both the equilibrium melting point of the crystallizing component and the crystal width. (b) At intermediate temperatures data are presented in favour of parallel but separate crystallization of the components. Crystallization of the low molecular weight component in the blend is promoted by the presence of high molecular weight substrate crystals. (c) At low temperatures partial cocrystallization is suggested based on data by TEM and d.s.c.

INTRODUCTION

Molecular fractionation is a well-known phenomenon accompanying the crystallization of polymers. In linear polyethylene (LPE), which is the most studied polymer in this respect, fractionation occurs due to differences in molecular weight[1-4]. The low molecular weight material crystallizes at low temperatures in subsidiary lamellae located between the dominant lamellae and in the spherulite boundaries[5,6]. The segregation of low molecular weight material has a major effect on the weakest-link properties of LPE[7-9]. Evidence has been presented for the location of fracture to domains of low molecular weight segregated material[7,9].

In 1974, Wunderlich and Mehta[1,2] summarized the experimental evidence for molecular fractionation in LPE and rationalized it in terms of a hypothesis in which a concept introduced by the authors, molecular nucleation, played a vital role. According to Wunderlich and Mehta, there exists at each temperature of crystallization (T) a critical molecular weight (M_{crit}) such that the molecules of molecular weight greater than $M_{crit}(T)$ are able to crystallize at T, whereas molecules of molecular weight less than $M_{crit}(T)$ are unable to crystallize. Most studies concerned with molecular fractionation deal with samples of a broad continuous molecular weight distribution (MWD). Crystallization kinetics of binary mixtures of narrow MWD fractions have been studied to a lesser degree. Crystallization of binary mixtures of LPE (molecular weight ranging from 1000 to 20 000) have been studied by Smith and St. John Manley[10] and, depending

on cooling rate, two types of crystallization have been indicated by these authors: (i) at low cooling rates, separate crystallization of the components occurred; (ii) water-quenched samples displayed only one melting peak and one SAXS peak which was taken as evidence for cocrystallization of the components. Gedde and Jansson[3] presented differential scanning calorimetry (d.s.c.) data in favour of a cooling rate dependence of molecular weight segregation in a broad MWD LPE.

This paper presents data on isothermal and constant rate cooling crystallization of binary mixtures of sharp LPE fractions in the molecular weight range of 2500–66 000. The question of separate crystallization or cocrystallization is addressed.

EXPERIMENTAL

Polarized microscopy. Crystallization was studied in the hot stage by cooling (10 K min⁻¹) the 10 mm thick

---

* Present address: Department of Physical Chemistry, Polymer Group, Basque Country University, 644 Bilbao, Spain
† To whom all correspondence should be addressed

samples from 450 K to the crystallization temperature (T) and by photographing at different times (t) after the establishment of isothermal conditions. A linear relationship was always established between the spherulite radius/axialite length and t, and by measurement of at least five growing spherulites/axialites per sample at each temperature a mean value for the linear growth rate (G) was determined. The linear growth rate data were further treated according to the equation derived by Hoffman et al.[12]:

$$G = G_0 \exp[-U^*/R(T - T_\infty)]$$
$$\exp[-Kb\sigma\sigma_e T_m^\circ/(k\Delta h_f T\Delta \mathit{Tf})] \tag{1}$$

where G_0 is a constant, U^* is the activation energy for short range transport of crystallizable units, T_∞ is a temperature which is related to T_g, K is an integer constant which is either 2 (regime II) or 4 (regime I), b is the monolayer thickness, σ is the lateral surface free energy, σ_e is the fold surface free energy, T_m° is the equilibrium melting temperature, Δh_f is the heat of fusion, ΔT is the supercooling and $f = 2T/(T_m^\circ + T)$ which is a correction factor taking into account changes in Δh_f with temperature. The thermodynamic data used are given at the end of the experimental section.

D.s.c. Samples weighing about 5 mg were cooled in the d.s.c. apparatus at a rate of 80 K min^{-1} from 450 K to the crystallization temperature (T) after which isothermal conditions were established and the crystallization exotherm was recorded. The samples were finally cooled from T to 280 K at a rate of 80 K min^{-1} and then heated from 280 to 450 K at a rate of 10 K min^{-1} while the melting was recorded. The thermal treatment described above is referred to as *isothermal crystallization* (IC). The crystallization data were treated according to equation (2) which is a d.s.c. equivalent of equation (1):

$$1/t_{0.5} = C \exp[-U^*/R(T - T_\infty)]$$
$$\exp[-Kb\sigma\sigma_e T_m^\circ/(k\Delta h_f T\Delta \mathit{Tf})] \tag{2}$$

where $t_{0.5}$ is the time at which 50% of the final crystallinity is obtained and C is a constant.

In order to study crystallization at greater degrees of supercooling, samples from one of the binary mixtures, L66/L2.5 (0.5/0.5), were either cooled at a constant rate (0–80 K min^{-1}) from the melt in the d.s.c. apparatus or quenched directly in an ice–water mixture. The melting of these samples was recorded in the d.s.c. at a heating rate of 10 K min^{-1}.

TEM. Three samples were studied by TEM: L66 and L66/L2.5 (0.5/0.5) quenched from 450 K in air and L66/L2.5 (0.5/0.5) after crystallization from the melt at 392 K for 3 h followed by a cooling to 300 K at a rate of 80 K min^{-1}. For both air-quenched samples it has been previously shown by d.s.c. that crystallization occurs at about 380 K[11]. Further details from the thermal treatment are given in another paper[11]. The samples were treated according to the Kanig method[13]: small pieces were treated with chlorosulphonic acid for 8 days at 308 K, stained with 0.7% uranyl acetate for 24 h at room temperature, embedded in epoxy and sectioned with a glass-knife-equipped LKB microtome at room temperature. The 80–100 nm thick sections were examined in a Jeol Jem 100B.

Thermodynamic data. The data used are: $\Delta h_f = 293$ kJ kg^{-1} (ref. 14); $T_m^\circ(L66) = 417.7$ K, $T_m^\circ(L22) = 416.4$ K, $T_m^\circ(L11) = 414.2$ K (all three determined from the Broadhurst equation assuming $T_m^\circ(M = \infty) = 418$ K[12]), $T_m^\circ(L2.5) = 398$ K (as determined from a $T_m - T_c$ plot), $U^* = 6.3$ kJ mol^{-1}, $T_\infty = 201$ K, $\sigma = 14.1$ mJ m^{-2}, $b = 0.415$ nm (ref. 12).

RESULTS AND DISCUSSION

Figure 1 illustrates the general features of the crystallization of the blends. Above a certain temperature (393 K in *Figure 1*), only one of the components (L66 in *Figure 1*) crystallizes. The crystallization in this temperature domain is referred to as *high temperature crystallization*. At lower temperatures (lower than 393 K in *Figure 1*), both components crystallize separately or in the same crystal lamellae. Crystallization in this temperature domain is referred to as *intermediate temperature* or *low temperature crystallization*. The border between these two is not well-defined as discussed later.

High temperature crystallization

For the analysis of the linear growth rate data in accordance with equation (1), it is necessary to know the equilibrium melting point of the crystallizing component. This is at present possible in only two cases: (a) crystals of the pure sharp fraction in equilibrium with a melt of the same composition (data are presented in the experimental section); (b) crystals of one of the components in a binary mixture in equilibrium with the melt containing the two completely miscible components. In the latter case the equilibrium melting point (T_m) for the crystallizing component in the binary mixture has been calculated according to the equation originally derived by Nishi and Wang[15] using the Flory–Huggins approximation:

$$1/T_m - 1/T_m^\circ = -(R/\Delta H_u)[(\ln v_2)/m_2$$
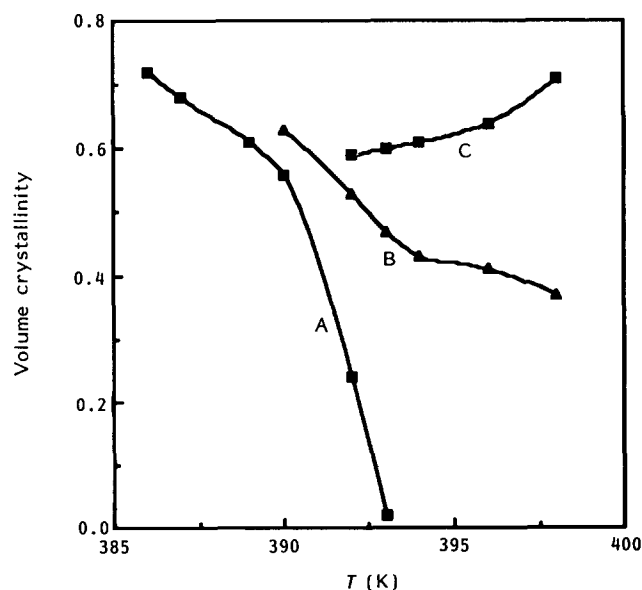$$+ (1/m_2 - 1/m_1)v_1 + \chi v_1^2] \tag{3}$$

Figure 1 Final volume crystallinity (at crystallization temperature, T) plotted as a function of crystallization temperature for L66 (C), L2.5 (A) and L66/L2.5 (0.5/0.5) (B)

where T_m° is the equilibrium melting point of the pure crystallizable component, ΔH_u is the heat of fusion per mole of repeating units, v_1 and v_2 are the volume fractions, m_1 and m_2 are the degrees of polymerization of uncrystallizable (at the particular temperature) and crystallizable component, respectively, and χ is the interaction parameter. Equation (3) assumes the complete miscibility of the two components in the melt and the complete immiscibility of the two components in the solid state, which is clearly fulfilled at low degrees of supercooling. The interaction parameter has to be determined which is not an easy task due to the problem of determining the equilibrium melting point. In plots of log G versus the crystallization temperature for the binary mixtures of L66/L2.5 (*Figure 2*), the curves are essentially parallel but shifted along the temperature axis. In the following analysis it is assumed that this shift in temperature is equivalent to a shift in equilibrium melting point. In a plot of the temperature corresponding to log $G = -3$ (*Figure 2*) versus composition, the best fit of the data yields a value for the interaction parameter of -0.008. Similar slightly negative values for the interaction parameter have been reported by Smith and St. John Manley[16].

Figure 3 presents the linear growth rate data treated according to equation (1) using the equilibrium melting point of L66 in the binary L66/L2.5 mixtures determined from equation (3). Data for L66 and the 0.5/0.5 mixture of L66/L2.5 fall essentially on the same curve, in both cases with a pronounced break in the curve at about 16.5 K supercooling. The slope of the high temperature part is greater by a factor of about two than the slope in the low temperature part which, for the pure sharp fraction (L66), is in accordance with what is expected for regime I and regime II crystallization[12]. The data for the 0.3/0.7 mixture of L66/L2.5 follow a similar curve, but the break point occurs at a higher degree of supercooling (17.5 K). The slope of the high temperature region (regime I) is the same as for the other samples shown in *Figure 3*. The low temperature part (regime II), on the other hand, has a
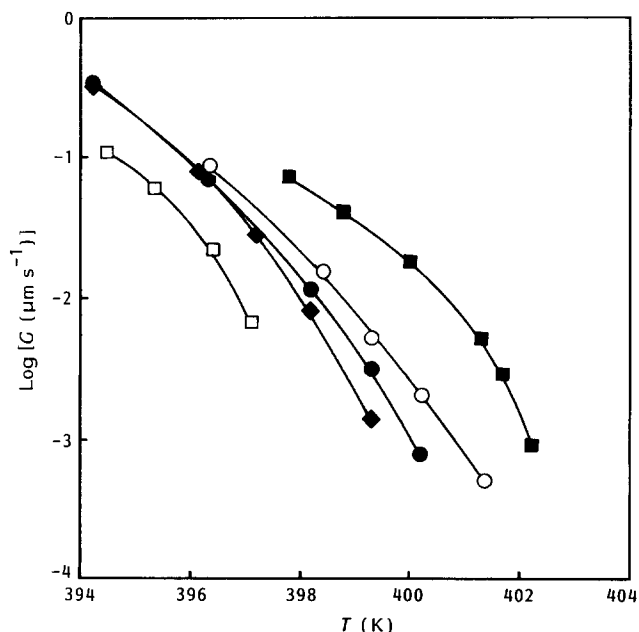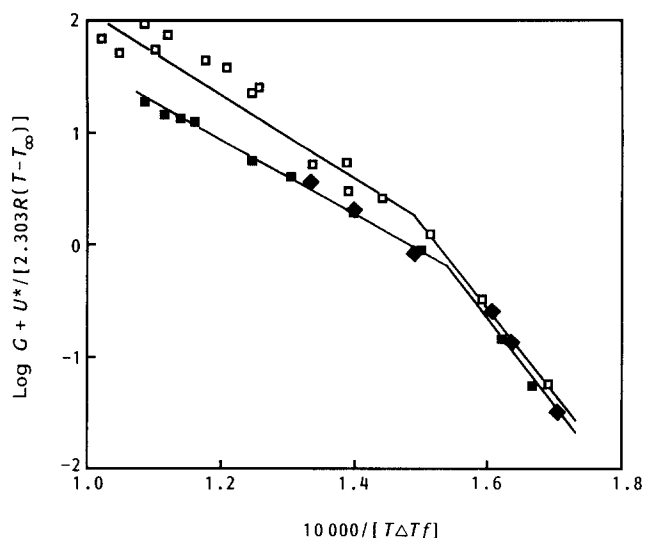

Figure 3 Plots of log G $(\mu m\,s^{-1}) + U^*/[2.303\,R(T - T_\infty)]$ vs. $1/(T\Delta Tf)$ for L66 (◆), L66/L2.5 (0.5/0.5) (■) and L66/L2.5 (0.3/0.7) (□). The quantities used are defined in the experimental section
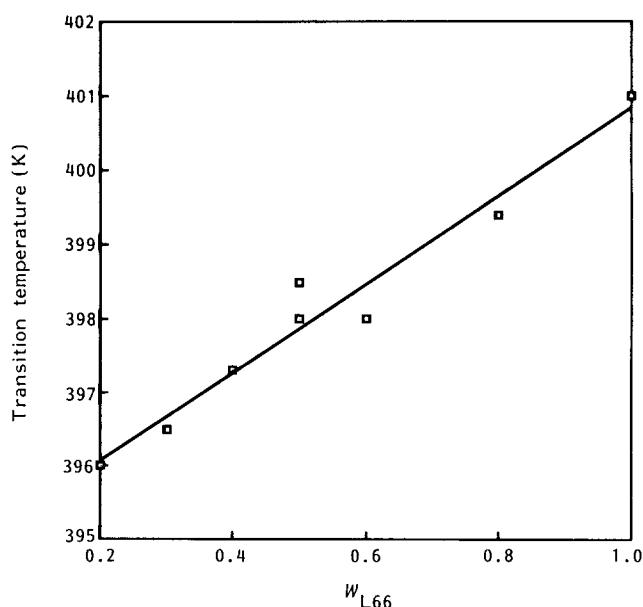

Figure 4 Temperature for axialite/spherulite transition plotted as a function of composition (w_{L66}) for blends of L66/L2.5

slightly steeper slope than that of L66 and L66/L2.5 (0.5/0.5). In accordance with the literature[12], it is shown by data from light microscopy and small angle light scattering presented in the accompanying paper[11] that the change in crystallization kinetics is accompanied by a change from an axialitic structure (regime I) to a non-banded spherulitic structure (regime II). Thus, the introduction of the low molecular weight component seems to have no major influence on the occurrence of the two regimes of crystallization or on the values for the slopes in the two regimes. The supercooling associated with the regime I–regime II transition is about 1 K greater for the blends rich in L2.5 ($w_{L66} = 0.2$–0.3) than for pure L66 (*Figure 4*). This minor change in transition supercooling may be explained within the framework of the Hoffman theory by a 50% reduction in the crystal substrate length in L66/L2.5 (0.2/0.8) with respect to that of L66. TEM work is at present being carried out to check this hypothesis.
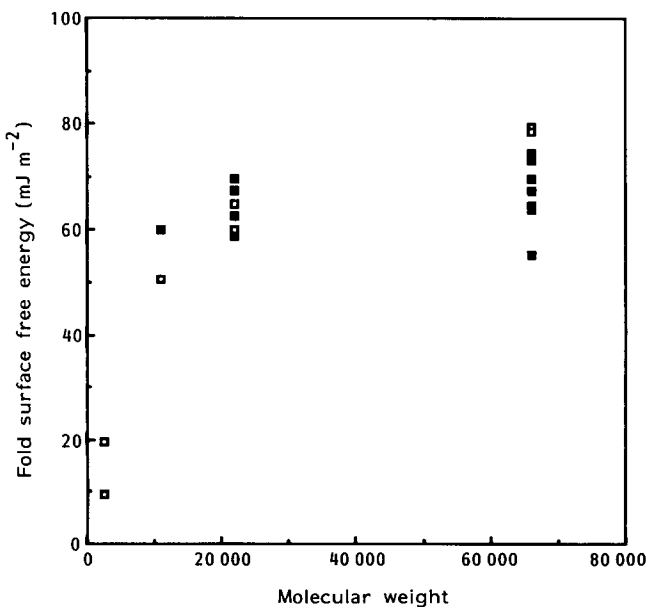

Figure 2 The logarithm of the linear growth rate (G) plotted as a function of crystallization temperature, T, for different binary mixtures of L66/L2.5: 1/0, ■; 0.8/0.2, ○; 0.6/0.4, ●; 0.4/0.6, ◆; 0.2/0.8, □

A summary of all crystallization rate data (including data from both polarized microscopy and d.s.c.) is presented in *Figure 5*. The molecular weight dependence of the fold surface free energy of the pure LPE fractions (*Figure 5*) follows earlier data by Hoffman *et al.*[12] More interesting, however, is the coincidence of fold surface free energy data from pure, sharp fractions and binary mixtures. A similarity in the nature of the fold surface of the two sets of samples is thus demonstrated. The minor lowering in the fold surface free energy observed in the L66 blends may be due to a limited cocrystallization of the components in the blends indicating the presence of higher molecular weight species in the low molecular weight components (L2.5, L11 and L22).

The temperature region in which single component crystallization occurs depends on the constituents. For binary mixtures of L66 and L2.5 it occurs at temperatures greater than 393 K.
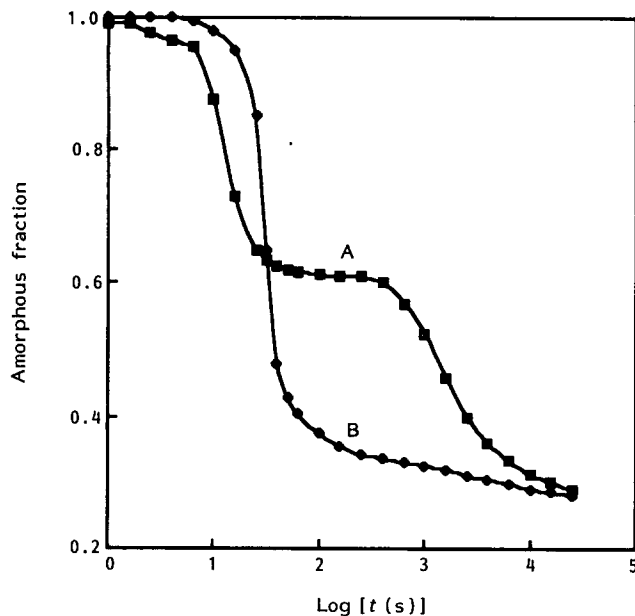
Intermediate temperature crystallization

Figures 6 and 7 demonstrate two important features of the crystallization of the binary mixtures at intermediate temperatures. Both L66 and L2.5 crystallize at 392 K but at considerably different rates, as can be seen in *Figure 6*. The crystallization of the 0.5/0.5 blend shows that the crystallization of L2.5 is promoted by the presence of L66. The crystallization of L66 in the binary blend is delayed compared with that of pure L66. The final degree of crystallinity in the binary mixture agrees with the value obtained from the pure components assuming simple additivity (*Figure 6*).

Figure 7 displays melting thermograms of L66/L2.5 (0.5/0.5) crystallized at 392 K from the melt for different periods of time and cooled at a rate of $80 \, \text{K} \, \text{min}^{-1}$ to 280 K. Samples crystallized at 392 K for only a short period of time (curve A), exhibit two melting peaks. The low temperature peak is associated with the crystals formed during the cooling phase. The high temperature peak is associated with the material crystallized at 392 K.

Figure 6 Amorphous fraction (from d.s.c.) plotted as a function of the logarithm of the crystallization time (*t*) for L66/L2.5 (0.5/0.5). (A) Calculated curve based on the crystallization of single components. (B) Measured curve for the blend
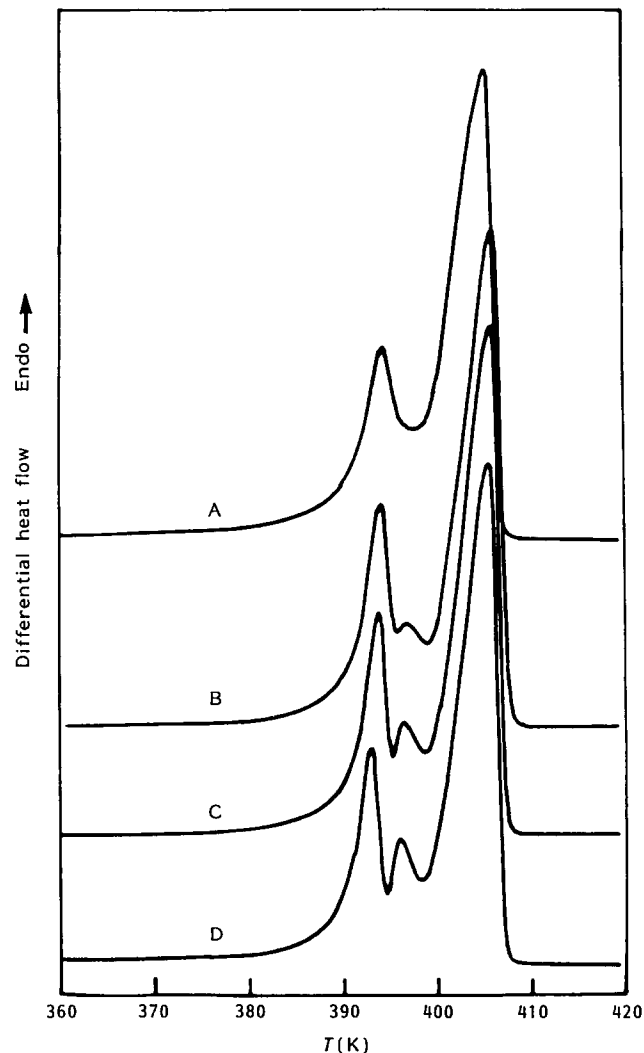
Figure 7 Melting endotherms of L66/L2.5 (0.5/0.5) crystallized at 392 K for different times (*t*) and then cooled at a rate of $80 \, \text{K} \, \text{min}^{-1}$: (A) $t = 468 \, \text{s}$; (B) $t = 11 \, 160 \, \text{s}$; (C) $t = 21 \, 600 \, \text{s}$; (D) $t = 45 \, 000 \, \text{s}$

Figure 5 Fold surface free energy (σ, obtained according to equation (1) applying linear growth rate data from polarized microscopy and d.s.c. data according to equation (2)) plotted *versus* molecular weight of crystallizing component. Single component samples (□) and binary 50/50 blends (■)

On prolonged isothermal treatment at 392 K, the high temperature peak is split into two peaks (curves B–D). The lower temperature peak of the two is invariant in both temperature and size and shows a perfect agreement in terms of temperature with the melting of extended-chain crystals of L2.5. The higher temperature peak occurs at progressively higher temperatures with prolonged time at 392 K, indicating isothermal thickening of folded-chain L66 crystals. Thus, at 392 K, crystallization of L2.5 in the L66/L2.5 blend is significantly promoted by the presence of L66 but evidently occurs in separate, subsidiary lamellae.

Further evidence for the occurrence of separate crystallization of the components was obtained by TEM (*Figure 8*). A very 'helpful' property of the L2.5 component is that it is not stainable with the Kanig method[17]. No contrast between the amorphous and crystalline phase is obtained. This has also been reported earlier by Stack *et al.*[18] on similar samples. Thus, the presence of isolated domains of L2.5 material in the blend should be easily distinguished as white spots. There is, however, another cause for the absence of contrast. If the stained surfaces of the crystal lamellae are tilted with respect to the beam their contours gradually disappear and the contrast is lost. However, by tilting the specimens it was established that this was not the case. The dominant feature of the L66/L2.5 (0.5/0.5) sample crystallized at 392 K for 3 h, shown in *Figure 8*, is the occurrence of relatively long and well-defined dominant lamellae surrounding areas apparently without lamellae. These dominant lamellae are most probably composed of material rich in L66 whereas the zones lacking lamellar structure obviously are composed of material rich in L2.5 forming non-stainable subsidiary lamellae. A striking feature of this sample is the holes inside the white zones (*Figure 8*) probably created by the sectioning process. This is due to the brittleness of L2.5 being a low molecular weight material.

Another item of importance can be seen in *Figure 3*. The crystallization of L2.5 at temperatures lower than 393 K in the L66/L2.5 mixture seems to have little or no effect on the kinetics as judged from the linear growth rate. The rate of crystallization of the dominant L66 lamellae evidently controls the propagation rate of the spherulite boundary.

Low temperature crystallization

Crystallization at low temperatures is experimentally difficult to perform for the obvious reason that it occurs so readily that low temperatures are not reached before the crystallization is completed. One way of performing this type of study is to cool the sample quickly and the crystallization may actually occur so rapidly that it can be considered to be pseudo-isothermal. Samples treated by so-called air-quenching, have been studied by TEM. The temperature at which these samples (L66 and L66/L2.5 0.5/0.5) crystallize is about 380 K, which corresponds to a supercooling of 36–38 K.

Careful examination of a number of micrographs taken from the L66/L2.5 sample shows that non-lamellar areas (see earlier in intermediate temperature crystallization) constitute only a very small part of the total sample area, of the order of a few per cent. The air-quenched L66/L2.5 sample also showed (*Figure 9a*) similar holes inside the white spots as the sample of the same composition crystallized at intermediate temperature (392 K). Holes of
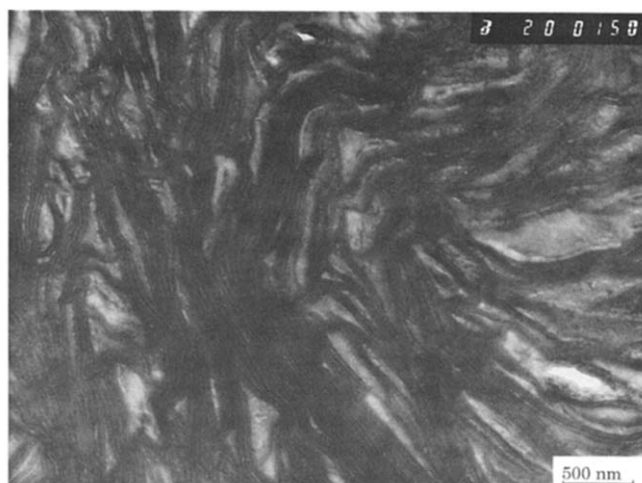

Figure 8 Transmission electron micrograph of L66/L2.5 (0.5/0.5) crystallized at 392 K for 3 h

this kind were absent in the L66 sample (*Figure 9c*). It should be pointed out, however, that this feature of holes is not dominant in the L66/L2.5 sample and that the concentration of cracks and L2.5-rich material is significantly lower in the air-quenched blend than in the corresponding sample crystallized at 392 K (cf. *Figures 8 and 9*).

Figure 10 presents the relevant information on the air-quenched samples gained by the TEM work. The crystal and amorphous layer thickness data are obtained from selected parts of micrographs showing a distinct lamellar contour. It is evident that both the crystal thickness and the amorphous layer thickness are lower in the blend than in the pure L66 sample. The thickness of the amorphous layer is 40% lower in the 0.5/0.5 blend than in L66. The crystal thickness is more moderately affected, being reduced by only 15%, by the introduction of L2.5 into L66. This is strong evidence in favour of an intimate mixing (cocrystallization) of the components in the air-quenched blend. The introduction of L2.5 into the L66 crystals is expected to reduce the amorphous layer thickness due to the simple fact that the L2.5 molecules will have a macroconformation which is either of extended-chain type or once and tightly folded. However, the presence in the micrographs of areas without lamellar features and not being tilted lamellae suggest that the cocrystallization is only partial. Thus, there is also a partial segregation of the components in the air-quenched blend.

In conclusion, binary blends based on L66 and L2.5 exhibit a partial cocrystallization when crystallized at 380 K. So far the data presented concern only blends crystallized at this particular temperature. It is however of interest to know the behaviour at other temperatures. By recording the melting of L66/L2.5 (0.5/0.5) samples crystallized during different constant cooling rates (0–80 K min⁻¹), the presence of two melting peaks was indicated independent of cooling rate. However, there is a significant overlap of the two peaks, particularly for the samples cooled at the higher rates. This cooling rate range corresponds to a crystallization temperature range from 386 to 392 K. The sample which was quenched directly into an ice–water mixture displayed only one melting peak. Thus, these d.s.c. data seem to indicate that the tendency to cocrystallization increases with increasing cooling rate, i.e. with decreasing crystallization temperature.
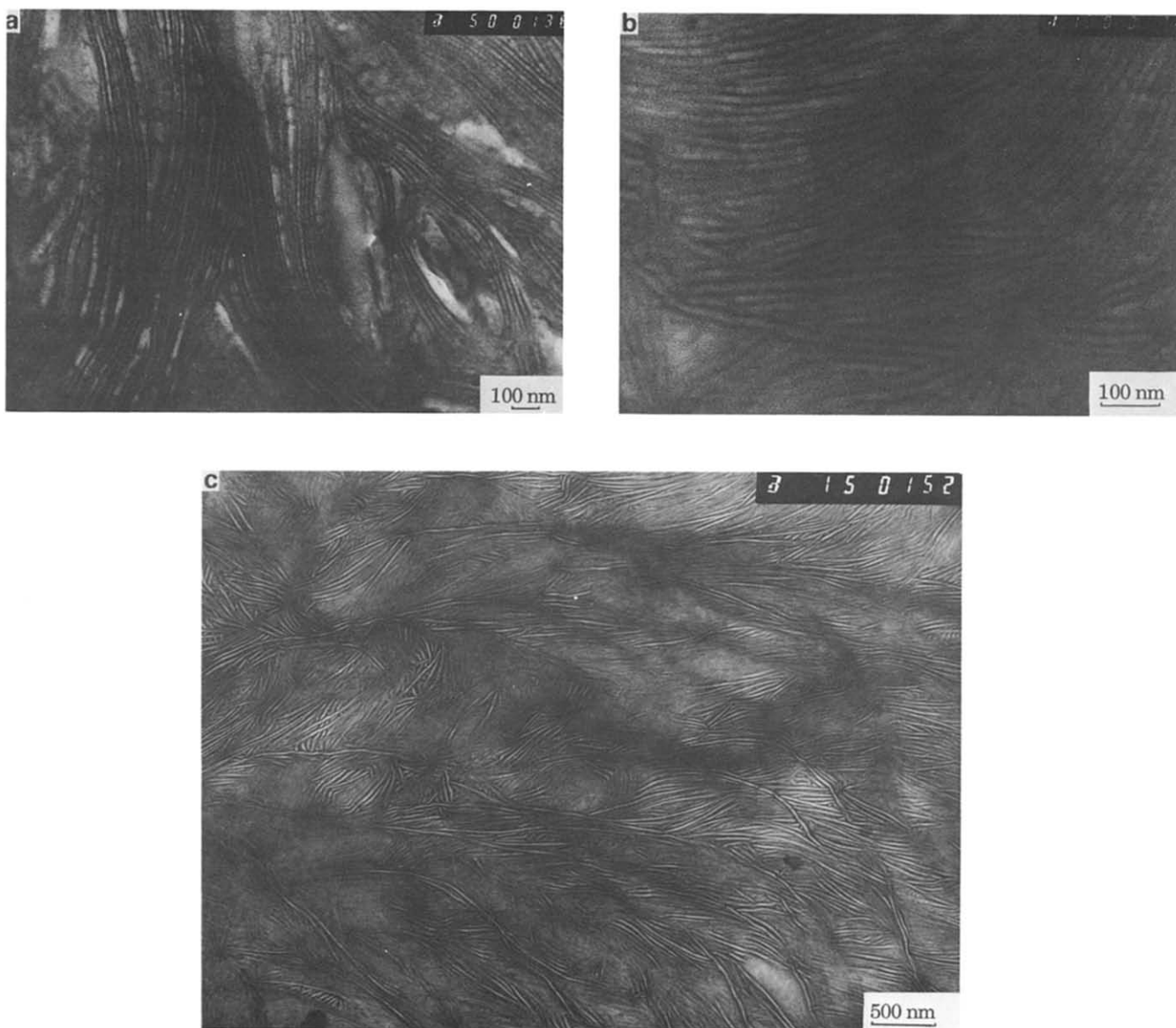
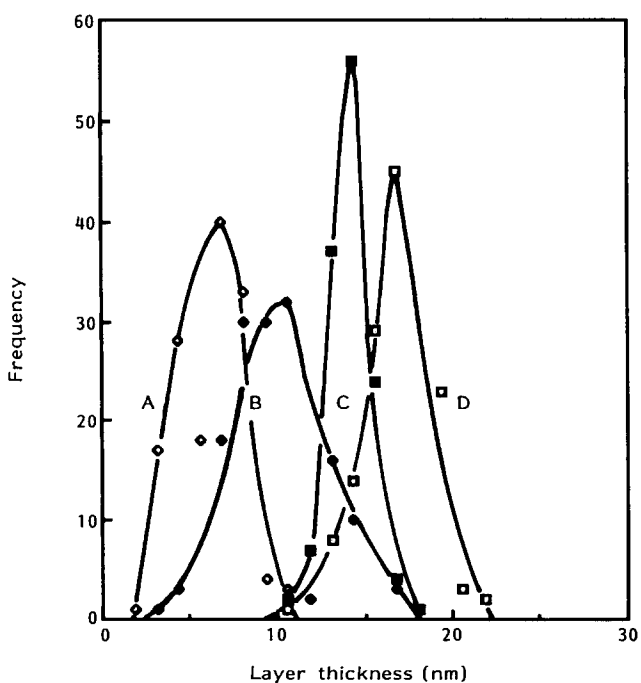**Figure 9** Transmission electron micrographs of air-quenched L66/L2.5 (0.5/0.5) (a and b) and L66 (c)

Figure 10 Thickness of amorphous layer (L_a) and crystal (l_c) of air-quenched L66/L2.5 (0.5/0.5) and L66 as revealed by TEM: (A) L_a — L66/L2.5 (0.5/0.5), $\langle L_a \rangle = 6.3$ nm; (B) L_a — L66, $\langle L_a \rangle = 10$ nm; (C) L_c — L66/L2.5 (0.5/0.5), $\langle L_c \rangle = 14.1$ nm; (D) L_c — L66, $\langle L_c \rangle = 16.6$ nm

CONCLUSIONS

Depending on the temperature, three types of crystallization have been observed in binary mixtures based on narrow MWD LPE ($M_w = 2500, 11\,000, 22\,000$ and $66\,000$):

At high temperatures, crystallization is confined to the high molecular weight component and the low molecular weight component is almost completely prohibited from entering the crystal phase. The introduction of a low molecular weight component (e.g. L2.5 into L66) has no significant effect on the nature of the fold surface. The occurrence of regime I and regime II crystallization is not affected by the presence of the low molecular weight component (e.g. L2.5 in L66). The degree of supercooling corresponding to the regime I/regime II transition is only moderately affected by the introduction of L2.5 into L66.

At intermediate temperatures, both components in the binary mixtures crystallize but evidently separately. The high molecular weight component (e.g. L66) crystallizes in dominant lamellae whereas the low molecular weight component (e.g. L2.5) crystallizes in subsidiary lamellae sandwiched between the dominant lamellae. The crystallization of the low molecular weight is promoted by the presence of high molecular weight substrate crystals in the binary mixtures.

At low temperatures, i.e. for L66/L2.5 (0.5/0.5) at 380 K, partial cocrystallization of the components in the binary blend takes place.

REFERENCES

1   Wunderlich, B. and Mehta, A. *J. Polym. Sci., Polym. Phys. Edn.* 1974, **12**, 255
2   Mehta, A. and Wunderlich, B. *Colloid Polym. Sci.* 1975, **253**, 193
3   Gedde, U. W. and Jansson, J-F. *Polymer* 1983, **24**, 1521
4   Gedde, U. W., Eklund, S. and Jansson, J-F. *Polymer* 1983, **24**, 1532
5   Gedde, U. W. and Jansson, J-F. *Polymer* 1984, **25**, 1263
6   Bassett, D. C. 'Morphology of Polymers', Proceedings of 17th Europhysics Conference on Macromolecular Physics, Prague, July 1985, Walter de Gruyter, Berlin, 1986
7   Phillips, P. J. and Patel, J. *Polym. Eng. Sci.* 1979, **18**, 943
8   Gedde, U. W. and Jansson, J-F. *Polymer* 1985, **26**, 1469
9   Gedde, U. W., Eklund, S. and Jansson, J-F. *Polym. Bull.* 1982, **9**, 90
10 Smith, P. and St. John Manley, R. *Macromolecules* 1979, **12**, 483
11 Rego Lopez, J. M. and Gedde, U. W. *Polymer* 1988, **29**, 1037
12 Hoffman, J. D., Frolen, L. J., Ross, G. S. and Lauritzen Jr, J. I. *J. Res. Natl. Bur. Stand. (A)* 1975, **6**, 671
13 Kanig, G. *Colloid Polym. Sci.* 1977, **255**, 1005
14 Wunderlich, B. 'Macromolecular Physics', Vol. 3, Academic Press, New York, 1980
15 Nishi, T. and Wang, T. T. *Macromolecules* 1975, **8**, 909
16 Smith, P. and St. John Manley, R. *Macromolecules* 1979, **12**, 483
17 Conde Braña, M. T., Terselius, B. and Gedde, U. W., unpublished data
18 Stack, G. M., Mandelkern, L. and Voigt-Martin, I. G. *Macromolecules* 1984, **17**, 321